International Congress
INTERPRAEVENT 2002 in the Pacific Rim - MATSUMOTO/JAPAN
Congress publication, volume 1, pp.113-124

A TWO LAYER SIMULATION MODEL UNIFYING DEBRIS FLOW AND SEDIMENT SHEET FLOW

Jun-ichiro Takahama[1], Yuichiro Fujita[2], Yasuhiro Kondo[3], and Kei Hachiya[4]

ABSTRACT

Present study deals with deposition-erosion process of debris flow including transition state between fully dispersed debris flow to sediment sheet flow. A two layer model is proposed here to unify theses two kind of flows. An "interface" is introduced between the upper layer which mainly consists of water and the lower layer of dense sediment mixture through mass, volume and momentum fluxes exist. The model is expressed with mass and volume conservation equations of both water and sediment including a relation by describing level change of immobile bed as well as momentum equations of the both layers. Numerical analyses of the model were carried out to explain experiments and calculated results agreed well with experimental data of wide range of deposition-erosion process of debris flow and sediment sheet flow.

KEYWORDS: debris flow, sediment sheet flow, deposition-erosion process, two layer model

INTRODUCTION

Prediction of sediment runoff caused by debris flows gives the most fundamental information to countermeasure planning. It is very important to evaluate affecting range and magnitude of the debris flow according to the initial-boundary condition such as inflow at the upper most reach, topographic feature of the subsequent channel and so on.

In deposition processes of the debris flows, their flowing state may change greatly, since the vertical profile of sediment concentration is influenced by the decrease in the bed slope. Therefore, the transitional state from the debris flow to the bedload is necessary to be analyzed by unified procedure. Takahashi et al. (2000) classified the each sediment transport state and proposed a method to analyze the flow process with individual resistance law for each state. Hirano, Hashimoto et al. (1997) obtained a sediment discharge function in these region and evaluated erosion-deposition processes by the spatial imbalance of sediment discharge. Egashira et al. (2000) derived an exact solution of vertical profile of velocity and concentration at an equilibrium state from constitutive equations of debris flow proposed by themselves to introduce correction factors for their vertical distribution of them and introduced the factors into the governing equations for the flow state from debris flow to sediment sheet flow.

1)Faculty of Engineering, Gifu Univeristy, 1-1 Yanagido, Gifu 501-1193, Japan (jtaka@cc.gifu-u.ac.jp)

2)River Basin Research Center, Gifu Univeristy, 1-1 Yanagido, Gifu 501-1193, Japan (yfjt@cc.gifu-u.ac.jp)

3)MIKUNIYA CORPORATION-OSAKA OFFICE, Kaigan-Dori 3-3-3, Minato-ku, Osaka, Osaka, 552-0022 Japan(kondoh@mikuniya.co.jp)

4)Nikken Consultants, Inc., 6-17-19 Shinbashi, Minato-ku, Tokyo 105-0004, Japan (hachiya@nikken-con.co.jp)

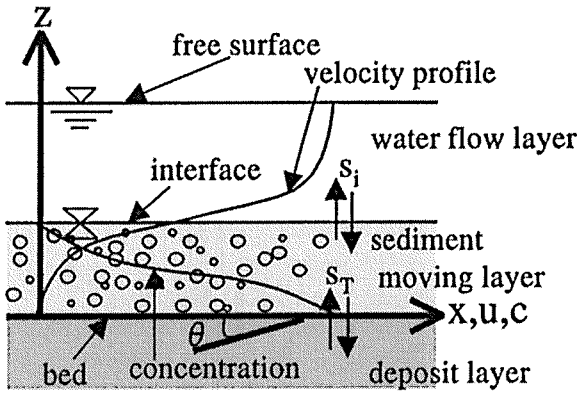

Fig.1 Schema of two layer flow model.

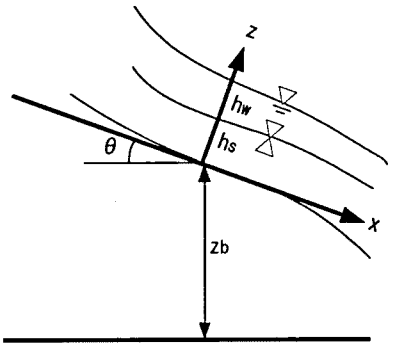

Fig.2 Coordinate system.

GOVERNING EQUATIONS OF A TWO LAYER MODEL

In the flow of compound materials in a steep channel as shown in Fig.1, two types of external forces are working as driving forces of the sediment layer: shearing force, which acts upon the interface between the two layers, and body force, which works inside the sediment layer.

From this perspective we can regard bed load as a flow in which the shearing force of the interface dominates, while debris flow is an opposite, where body force dominates and interface coincides free surface. Egashira et al. (1997) derived the relationship between the two external forces at the equilibrium state and evaluated the sediment discharge and velocity distribution in the sediment layer.

The water flow layer appears in the upper part of the sediment moving layer, then the flow undergoes transition from debris flow to sediment sheet flow. During this process, there exists the water flux through the surface of sediment moving layer to the upper layer. Inversely, the water flux to the lower layer through the interface of two layers appears at transition from the sediment sheet flow to the debris flow. In the non-stationary conditions of debris flow and sheet flow, as it is shown in Fig.1, the flux of mass and volume through interface intervenes. The flux from the sediment moving layer to the water flow layer is interpreted as source term in the equation for mass conservation of water flow layer. Let s_I be the source term according to flux across the interface, and using the coordinate system shown in Fig. 2, volume conservation law on the both layer and sediment concentration can be expressed as follows:

$$\frac{\partial h_w}{\partial t}+\frac{\partial (v_w h_w)}{\partial x}=s_I \qquad (1)$$

$$\frac{\partial h_s}{\partial t}+\frac{\partial (v_s h_s)}{\partial x}=s_T-s_I \qquad (2)$$

$$\frac{\partial (c_s h_s)}{\partial t}+\frac{\partial (\gamma c_s v_s h_s)}{\partial x}=c_* s_T \qquad (3)$$

in which h_w is the water flow layer depth, v_w is the depth averaged velocity of the water flow layer, h_s is the flow depth of sediment moving layer, v_s is the depth averaged velocity of the sediment moving layer, c_s is the mean concentration of sediment moving layer, c_* is concentration of deposit layer. s_T is the erosion rate and γ is the correction factor corresponding to the vertical distribution of velocity and concentration of the sediment moving layer as:

$$\frac{\partial z_b}{\partial t}=-\frac{s_T}{\cos\theta} \qquad (4)$$

$$\gamma=\frac{\int_0^{h_s} cu\,dz}{c_s v_s h_s} \qquad (5)$$

in which z_b is the bed height, θ is the bed slope, and c is the distributed concentration

distribution and u is velocity at any depth of the sediment moving layer.

Mass exchange between two layers through the interface is accompanied by the exchange of the momentum with the velocity at the interface. Momentum Equations of both layers are obtained as follow:

$$\frac{\partial(\rho_w v_w h_w)}{\partial t}+\frac{\partial\left(\rho_w \beta_w {v_w}^2 h_w\right)}{\partial x}-\rho_w s_I u_I=\rho_w g h_w \sin\theta-\frac{\partial P_w}{\partial x}-p_I\frac{\partial h_s}{\partial x}-\tau_w \tag{6}$$

$$\frac{\partial(\overline{\rho_s}\gamma' v_s h_s)}{\partial t}+\frac{\partial(\overline{\rho_s}\beta_s {v_s}^2 h_s)}{\partial x}+\rho_w s_I u_I=\rho_s g h_s \sin\theta-\frac{\partial P_s}{\partial x}+p_I\frac{\partial h_s}{\partial x}+\tau_w-\tau_b \tag{7}$$

in which ρ_w is density of the water flow layer, $\overline{\rho_s}$ is depth averaged density of sediment moving layer, u_I is velocity at the interface, P_W is integrated pressure over the water flow depth, P_s is that of sediment moving layer, p_I is pressure at the interface ($p_I=\rho_w g h_w \cos\theta$), τ_w is shear stress at the interface, τ_b is that at the bed. γ', β_w and β_s are correction factors according to vertical profile of the flow properties defined as following equations, respectively.

$$\gamma=\frac{\int_0^{h_s}\rho_s u\,dz}{\overline{\rho_s} v_s h_s} \tag{8}$$

$$\beta_s=\frac{\int_0^{h_s}\rho_s u^2 dz}{\overline{\rho_s}{v_s}^2 h_s} \tag{9}$$

$$\beta_w=\frac{\int_0^{h_w}u^2 dz}{{v_w}^2 h_w} \tag{10}$$

In this study, the x axis has been set along riverbed and the hydrostatic pressure distribution was assumed, which corresponds to neglect the terms caused by the curvature of the riverbed. Unity is arranged to the above-mentioned correction factors in the analysis:

$$\frac{\partial M_w}{\partial t}+\frac{\partial(v_w M_w)}{\partial x}-s_I u_I=g h_w \sin\theta-g h_w\cos\theta\frac{\partial(h_w+h_s)}{\partial x}-\frac{\tau_w}{\rho_w} \tag{11}$$

$$\frac{\partial M_s}{\partial t}+\frac{\partial(v_s M_s)}{\partial x}+\left\{\left(\frac{\rho_{s*}}{\overline{\rho_s}}-1\right)s_T+\left(1-\frac{\rho_w}{\overline{\rho_s}}\right)s_I\right\}v_s+\frac{\rho_w}{\overline{\rho_s}}s_I u_I=g h_s\sin\theta-g h_s\cos\theta\frac{\partial h_s}{\partial x}-\frac{\rho_w}{\overline{\rho_s}}g h_s\cos\theta\frac{\partial h_w}{\partial x}-\frac{1}{2\overline{\rho_s}}g{h_s}^2\cos\theta\frac{\partial\rho_s}{\partial x}+\frac{\tau_w}{\overline{\rho_s}}-\frac{\tau_b}{\overline{\rho_s}} \tag{12}$$

in which $M_w=v_w h_w$, $M_s=v_s h_s$.

RESISTNCE LAW AND EROSION-DEPOSITON RATE FOR THE ANALYSIS

Shear stresses, τ_w, τ_b, erosion rate, s_T, and exchange rate of volume through the interface, s_I, should be evaluated in order to close the governing equations. In this study, constitutive equations and erosion-deposition rate produced by Egashira et al. (1984,1997) are adopted, and, in addition, following approximations and assumptions are introduced.

(1) The bulk density of the sediment moving layer is vertically uniform, and can be postulated as $c_s=c_*/2$

(2) In the sediment moving layer, the ratio, α, between the pressure due to the energy conserved particle collision, p_d and the particle structural pressure p_s is regarded to be constant ($p_d/p_s=\alpha$), and to be naught at the river bed, that is $\alpha=0(p_d=0)$.

(3) Whole layers are handled as the sediment moving layer, when thickness of the sediment moving layer calculated from (1) exceeds total layer thickness. In this case, concentration of the sediment moving layer is allowed to become $c_s>c_*/2$.

From (1) and (2), s_I can be calculated from Eqs. (1) and (2), if the erosion-deposition rate,

s_T is determined.

Shear stress at the interface, τ_w is evaluated from a formula proposed by Egashira et al. (1997):

$$\frac{u(z)}{u_{*w}} = \frac{u_I}{u_{*w}} + \frac{1}{\kappa}\ln\left(\frac{z-h_s+\eta_0}{\eta_0}\right) \tag{13}$$

in which u_{*w} is the shear velocity defined by $\sqrt{gh_w\sin\theta}$, κ is Karman's constant and η_0 is length scale defined as

$$\eta_0 = \sqrt{k_f}\left(\frac{1-c_s}{c_s}\right)^{1/3} d \tag{14}$$

where k_f is an empirical constant, d is the sediment particle size and c_i is the sediment concentration at the interface specified as 0.05. In this study, average concentration $c_s = c_*/2$ of the sediment layer given to c_i with assumption of (1), that is $c_i = c_s$. Using the mean velocity of the water flow layer and velocity at the interface, τ_w is given by the following equations.

$$\tau_w = \rho_w f_w |v_w - u_I|(v_w - u_I) \tag{15}$$

$$f_w = \left[\frac{1}{\kappa}\left\{\left(1+\frac{\eta_0}{h_w}\right)\ln\left(1+\frac{h_w}{\eta_0}\right)-1\right\}\right]^{-2} \tag{16}$$

The constitutive equation of Egashira et al. (1997) is applied to the shear stress at the bed under the assumption of the uniform concentration. Momentum equation in the uniform flow condition is obtained as

$$\tau = \tau_{ext} \tag{17}$$

in which

$$\tau_{ext} = \tau_w + \{(\sigma-\rho_w)c_s\}g(h_s-z)\sin\theta \tag{18}$$

$$\tau = \tau_y + \tau_d \tag{19}$$

and τ is the internal shear stress, τ_{ext} is the shear stress due to external forces, τ_y is the yield shear stress, τ_d is dynamic shear stress due to turbulence of pore water between the particles and inelastic collision of the particles. The assumptions and simplifications above-mentioned yield the following equations for τ_y and τ_d:

i) at the bed

$$\tau_y = (\sigma-\rho_w)c_s g(h_s-z)\cos\theta\tan\phi \tag{20}$$

$$\tau_d = 0 \tag{21}$$

ii) within the sediment moving layer

$$\tau_y = (\sigma-\rho_w)c_s g(h_s-z)\cos\theta\frac{1}{1+\alpha}\tan\phi \tag{22}$$

$$\tau_d = \rho_w k_f \frac{(1-c_s)^{5/3}}{c_s^{2/3}} d^2\left(\frac{\partial u}{\partial z}\right)^2 + \sigma k_d(1-e^2)c_s^{1/3}d^2\left(\frac{\partial u}{\partial z}\right)^2 \tag{23}$$

in which σ is the density of the particle, e is the coefficient of restitution, ϕ_s is the friction angle and k_d is an empirical constant. Though α is a function of the concentration origunally, in this analysis the constant value ($\alpha = 0.25$) which Ashida, Egashira et al.(1984) gave approximately by the experiment.

Eqs. (17)-(21) give the ratio of h_s to the whole layer thickness, $h_t = h_s + h_w$ as the following equation, since τ_w is equal to $\rho_w g h_w \sin\theta$ at an equilibrium state.

$$\frac{h_s}{h_t}=\frac{\tan\theta}{(\sigma/\rho-1)c_s(\tan\phi-\tan\theta)} \tag{24}$$

Fig. 3 compares calculated values by equation (24) of the ratio between sediment layer thickness h_s to total flow depth h_t to experimental ones by Takahashi (1982) and Egashira, et al. (1990). As bed slope increases, so does h_s/h_t, in both of the experimental and calculated values. However, the distributive form of the experimental values shows to be upwardly convex, while the calculated values are convex in the downward direction, that is, they show the opposite trend. This is probably due to assumption of the uniform density in the calculations. It seems however to be able to ensure the accuracy for the practical use of approximate solution, because calculated values agree with the experimental value.

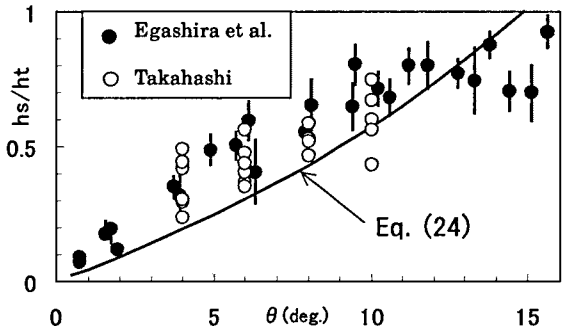

Fig.3 Calculated and experimental values for h_s/h_t.

By determining the sediment flow depth h_s shown in Fig.3 from Eqs. (17)-(23), the velocity distribution in the sediment layer can be obtained as shown in Fig. 4(a), (b), and (c), and the vertical distributions of $(\tau_{ext}-\tau_y)$ increase, constant, and decreases along the z axis respectively as the bed slope increases; corresponding to the three tendencies, the velocity distribution is upwardly convex, a straight line, and downward convex. Then, as shown in Fig. 4(a), when flow is fully dispersed debris flow, $(\tau_{ext}-\tau_y)$ becomes a triangular distribution, and the differential equation for velocity distribution is induced as the following equations from Eqs. (17)-(23):

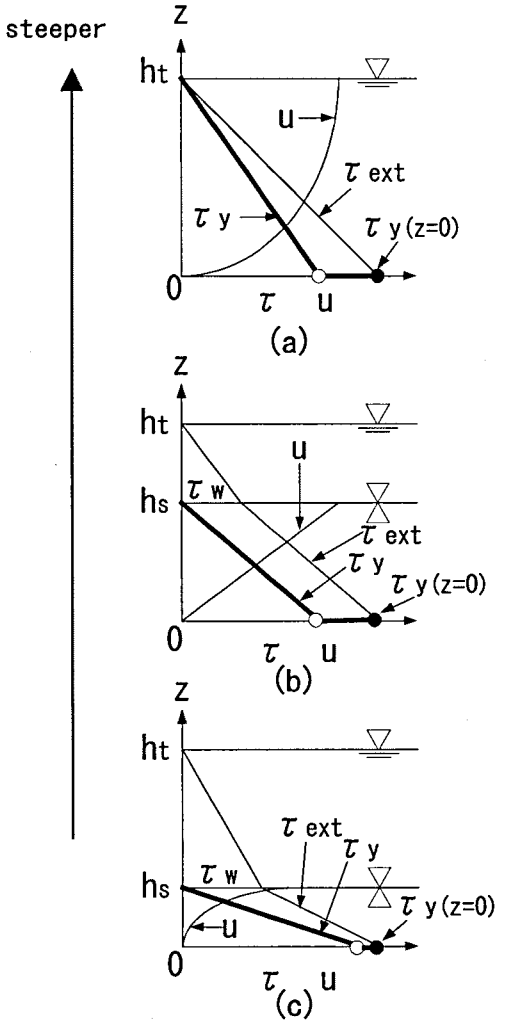

Fig.4 Stress and velocity distribution of the two layer model.

$$\frac{\partial\tilde{u}}{\partial\tilde{z}}=\frac{h_s}{d}\left\{\frac{W+G_{yk}(1-\tilde{z})}{f(c_s)}\right\}^{1/2} \tag{25}$$

$$f(c_s)=k_f\frac{(1-c_s)^{5/3}}{c_s^{2/3}}+k_d\frac{\sigma}{\rho_w}(1-e^2)c_s^{1/3} \tag{26}$$

$$W=\frac{\tau_w}{\rho_w g h_s}=\frac{f_w|v_w-u_1|(v_w-u_1)}{g h_s} \tag{27}$$

$$G_{yk}=\frac{\tau_{ext(z=z_b)}-\tau_{yk(z=z_b)}}{\rho_w g h_s}=\{(\sigma/\rho_w-1)c_s+1\}\sin\theta-(\sigma/\rho_w-1)c_s\cos\theta\frac{1}{1+\alpha}\tan\phi \tag{28}$$

in which $\tilde{u}=u/\sqrt{gh_s}$, $\tilde{z}=z/h_s$.

Based on equation (25), shear stress at the bed is given as the following equation:

$$\tau_b=(\sigma-\rho_w)c_s g h_s\frac{1}{1+\alpha}\cos\theta\tan\phi+\rho_w f_s|v_s|v_s \tag{29}$$

in which f_s is the friction factor of the sediment moving layer. Shear stress τ_w at the

interface is considered driving force (external force) for the sediment moving layer, τ_w shown in Eq. (15) is used in the calculation of the friction factor of the sediment moving layer and velocity at the interface. Accordingly, mean velocity, v_s, friction factor, f_s and u_I are given for the three case of the following equations from Eq. (24) and Fig. 4.

i) $h_w = 0$ (in case of (a) in Fig.4.)

$$\frac{v_s}{\sqrt{gh_s}} = \frac{2}{5}\frac{h_s}{d}\left\{\frac{G_{yk}}{f(c_s)}\right\}^{1/2} \quad (30) \qquad f_s = \frac{25}{4} f(c_s)\left(\frac{h_s}{d}\right)^{-2} \quad (31) \qquad u_I = \frac{5}{3} v_s \quad (32)$$

ii) $h_w > 0$ and $G_{yk} = 0$ (in case of (b) in Fig.4.)

$$\frac{v_s}{\sqrt{gh_s}} = \frac{1}{2}\frac{h_s}{d}\left\{\frac{W}{f(c_s)}\right\}^{1/2} \quad (33) \qquad f_s = 4 f(c_s)\left(\frac{h_s}{d}\right)^{-2} \quad (34) \qquad \frac{u_I}{v_s} = 2 \quad (35)$$

iii) $h_w > 0$ and $G_{yk} \neq 0$ (in case of (c) in Fig.4.)

$$\frac{v_s}{\sqrt{gh_s}} = \frac{4}{15}\frac{h_s}{d}\frac{1}{f(c_s)^{1/2} G_{yk}^{\,2}}\left\{W^{5/2} - \left(W + G_{yk}\right)^{3/2}\left(W - \frac{3}{2}G_{yk}\right)\right\} \quad (36)$$

$$f_s = \frac{225}{16} f(c_s) G_{yk}^{\,4}\left(W + G_{yk}\right)\left\{W^{5/2} - \left(W + G_{yk}\right)^{3/2}\left(W - \frac{3}{2}G_{yk}\right)\right\}^{-2}\left(\frac{h_s}{d}\right)^{-2} \quad (37)$$

$$\frac{u_I}{v_s} = \frac{5}{2} G_{yk} \frac{\left(W + G_{yk}\right)^{3/2} - W^{3/2}}{W^{5/2} - \left(W + G_{yk}\right)^{3/2}\left(W - \frac{3}{2}G_{yk}\right)} \quad (38)$$

In case ii) and iii) shown above by Eqs. (33), (36),(37) and (38), in the calculation procedure there can be some case in which the yield stress surpasses external force within the sediment layer or on the bed. The stress distribution must be corrected in such case to release the uniform flow approximation, as shown in Fig.5(a)(b).

(a) In the case of $G_{ys} \geq 0$ in which the body force acting inside of the sediment layer surpasses yield stress at the bed ,

if $W < 0$ then

$$W = 0; \quad (39)$$

where

$$G_{ys} = \{(\sigma/\rho_w - 1)c_s + 1\}\sin\theta - (\sigma/\rho - 1)c_s \cos\theta \tan\phi. \quad (40)$$

(b) In the case of $G_{ys} < 0$ in which the body force is smaller than yield stress,

if $W + G_{ys} < 0$ then

$$W = -G_{ys}. \quad (41)$$

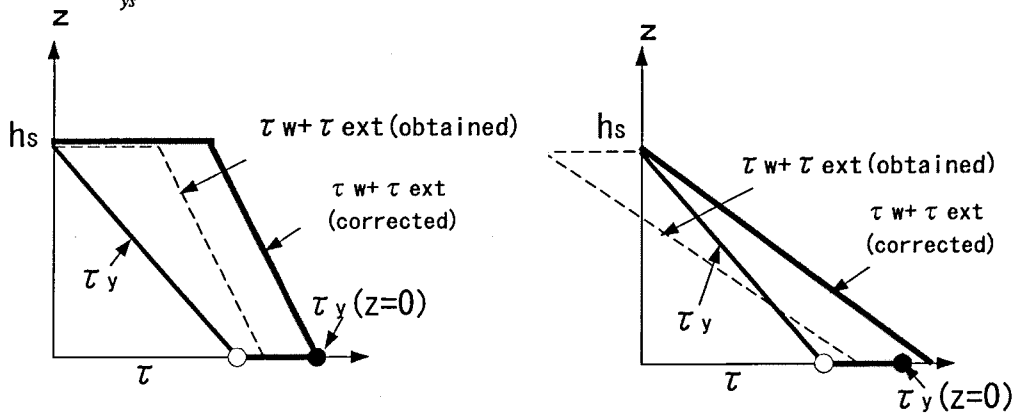

Fig.5 Correction of the stress profile in the calculation procedure of the two layer model.

The stress state shown as the Fig.5(a) appears when debris flow goes into still water zone, while that shown as the Fig.5(b) arises when pressure gradient in the water flow layer is the reverse to the direction of the flow.

The erosion-deposition rate by Egashira et al. (1988) was expanded to present a two layer model:

$$s_T = v_t \tan(\theta - \theta_e) \tag{42}$$

in which v_t is total depth averaged velocity, θ_e is the equilibrium bed slope for the averaged concentration for whole flow, which is obtained by momentum balance at the bed.

$$v_t = v_s \frac{h_s}{h_t} + v_w \frac{h_w}{h_t} \tag{43}$$

$$\tan\theta_e = \frac{(\sigma/\rho_w - 1)c_t}{(\sigma/\rho_w - 1)c_t + 1} \tan\phi \tag{44}$$

$$c_t = c_s \frac{h_s}{h_t} \tag{45}$$

Influence of the assumptions and approximations fro the simplicity on the analysis accuracy are examined before the simulation is carried out for complicated condition. Namely, the calculated results of the sediment discharge function and velocity coefficient are compared with the experimental values, and the validity is examined.

Sediment discharge rate per unit width rate, q_b is obtained as $q_b = v_s c_s h_s$, and its non-dimensional form becomes to be proportional to $\tau_*^{5/2}$ (τ_* is the non-dimensionally shear stress), as shown in the following equation.

$$\Phi = K_0(\sigma/\rho - 1)^{1/2} \left\{ \frac{1}{\cos\theta(\tan\phi - \tan\theta)} \right\}^{5/2} c_s^{-3/2} \tau_*^{5/2} \tag{46}$$

in which $\Phi = q_b / \sqrt{(\sigma/\rho - 1)gd^3}$, $\tau_* = \frac{gh_t \sin\theta}{(\sigma/\rho - 1)gd}$ and K_0 is obtained as the following equation to the condition of G_{yk}.

(a) $G_{yk} \neq 0$

$$K_0 = \frac{4}{15} \frac{1}{f(c_s)^{1/2} G_{yk}^{\ 2}} \left\{ W^{5/2} - (W + G_{yk})^{3/2} \left(W - \frac{3}{2} G_{yk} \right) \right\} \tag{47}$$

(b) $G_{yk} = 0$

$$K_0 = \frac{1}{2} \left\{ \frac{W}{f(c_s)} \right\}^{1/2} \tag{48}$$

Fig. 6 shows the experimental values of sediment discharge by Egashira et al. (1990) and these calculated from Eq. (46) using the experimental total flow depth h_t. Since no significant differences are not caused by bed slope in the calculated values, the figure shows only two examples for $\theta = 2$ and $\theta = 8$ degrees. The materials used in the experiment were uniform sands of $d_{50} = 0.144cm$ and $d_{50} = 0.368cm$, and the bed slopes were ranged from 0.72 to 15.6 degrees. A comparison of calculated and experimental values shows good agreement expect for the case where the latter become somewhat larger than the former when the calculated value h_s/d by Eq. (24) is less than 1.

From the experimental data used in Fig.6, those satisfying the condition of $h_s/d \geq 1$ were adopted to examine velocity coefficient as shown in Fig.7. The gradient of the velocity coefficient in the calculation decreases as the bed slope becomes mild. The calculated values of velocity coefficient for mild slope exceed that for steep slope as increase of h_t/d. The calculated values of velocity coefficient increase with decrease of bed slope in the range of

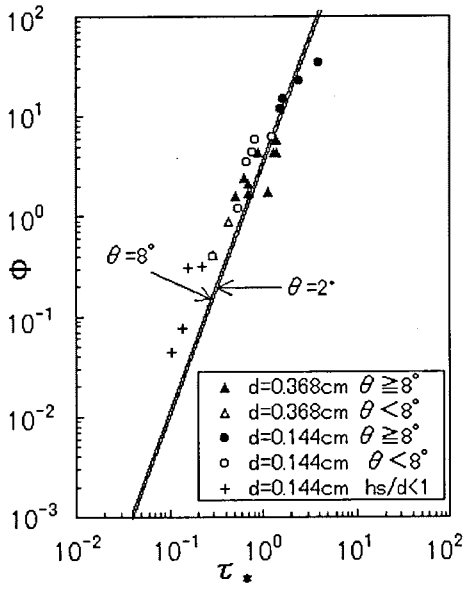

Fig.6 Calculated and experimental Values for sediment dischrage.

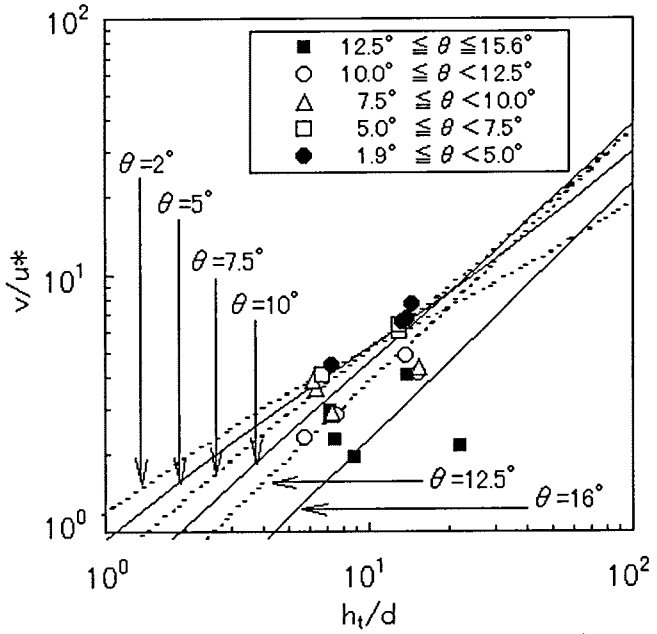

Fig.7 Calculated and experimental values for u/u_*.

experimental values of h_t/d where experimental results show same tendency. From these comparisons, introduced approximations and assumptions are appropriate, because values can be explained by this model, and analysis accuracy can be expected. By separating the governing equations to the two layers, unified analysis becomes possible for the flow in which all layers are the water flow from the flow in which all layers are the sediment moving layer.

APPLICATION OF THE TWO LAYER MODEL TO DEPOSITION-EROSION PROCESES OF DEBRIS FLOWS

The experiment on deposition-erosion processes of debris flow was carried out in a rectangular channel having an abrupt slope reducing (Takahama, Fujita et al.(2002)) and its were compared with those calculated by the two layer model. In the experiment, uniform sand (d=0.342cm) was supplied, and it was also used as the roughness element of the channel bed. In each run, the sand and water of certain quantity were supplied during the prescribed time, as shown Table 1 of the experimental conditions. In the table, "upstream" and "downstream" in the table indicate the upstream and the downstream reach from the abrupt reduction point of bed slope, and the upstream reach is fixed to 18 degrees. "R" in the table indicates the rigid bed, and

Table 1 Experimental conditions.

Run No.	Upstream	Downstream		qs	qw	c	time
	state	state	gradinent	(cm^2/s)	(cm^2/s)		(sec.)
1-1-1	R	R	2°	39.2	89.7	0.304	5.30
1-1-2	R	R	2°	46.8	88.4	0.346	6.02
1-1-3	R	R	2°	55.5	80.7	0.407	6.15
1-1-4	R	R	2°	55.5	81.6	0.405	7.11
1-2-1	R	R	4°	39.2	88.8	0.306	5.90
1-2-2	R	R	4°	44.4	82.9	0.349	10.88
1-2-3	R	R	4°	55.5	84.2	0.397	11.41
1-2-4	R	R	4°	55.5	84.6	0.396	5.81
1-3-1	R	R	8°	35.6	82.3	0.302	10.86
1-3-2	R	R	8°	44.4	82.4	0.350	5.68
1-3-3	R	R	8°	55.5	81.7	0.405	6.68
2-1-1	R	M	2°	37.7	88.1	0.300	10.49
2-1-2	R	M	4°	51.5	76.2	0.403	10.42
2-2-1	R	M	2°	37	85.6	0.302	10.85
2-2-2	R	M	4°	54.6	84.7	0.392	11.24
3-1-1	M	M	2°	40.6	93.3	0.303	10.26
3-1-2	M	M	4°	38.6	90.2	0.300	10.71

"M" indicates the movable bed fully saturated, and q_s and q_w are respectively inflow rates of sediment and water per unit time and per unit width, and supply duration time of the mixture is listed in the column at the right end. In the case of Run1-1-4 and Run1-2-4, after water-sediment mixture was supplied for the time, supply of sediment was stopped and only the water supply was continued for 14.4 and 3.30 seconds respectively. Numerical simulations were carried out by Leap-Frog Scheme.

Experiment and analysis of deposition process of debris flows

In Fig.8, Calculated results are shown being compared with flume data on time variations of the longitudinal profiles of interface or surface of sediment moving layer as well as those of the terminal bed calculations. In some case, the results show that all layers of the flow were handled as a sediment moving layer as those in one layer model. The moment at which the debris flow reached the point of abrupt slope reducing has been defined that t=0 second. X-axis set along the bed of the downstream reach is made to be in quadrature axis, and the point of abrupt slope reducing is defined as the origin of the x-coordinate. Triangle in the figure indicates the interface between two layers or the surface of sediment moving layer in the experiment, and square the immobile bed profile. Circle indicates the front of the water flow, only in case that its location can be confirmed by video records. For the calculation results, broken line indicates free surface, thin line the interface between two layers in a two-layer model, and the bold line the immobile bed profile. In the experiment, the water flow layer appeared when deposition of the debris flow began, and the water flow layer formed the front of the flow. In the two-layer flow model, this process can be expressed as water flow layer separates from the sediment moving layer, and the front of water flow and interface between two layers came out. The terminal bed profile in the calculation can also express those in the experiment considerably. On the other hand, in one layer model, a sediment moving layer proceed with rather low velocity and deposits easily. Thus the changes in sediment flowing state and resistance of the flow in deposition process cannot be expressed.

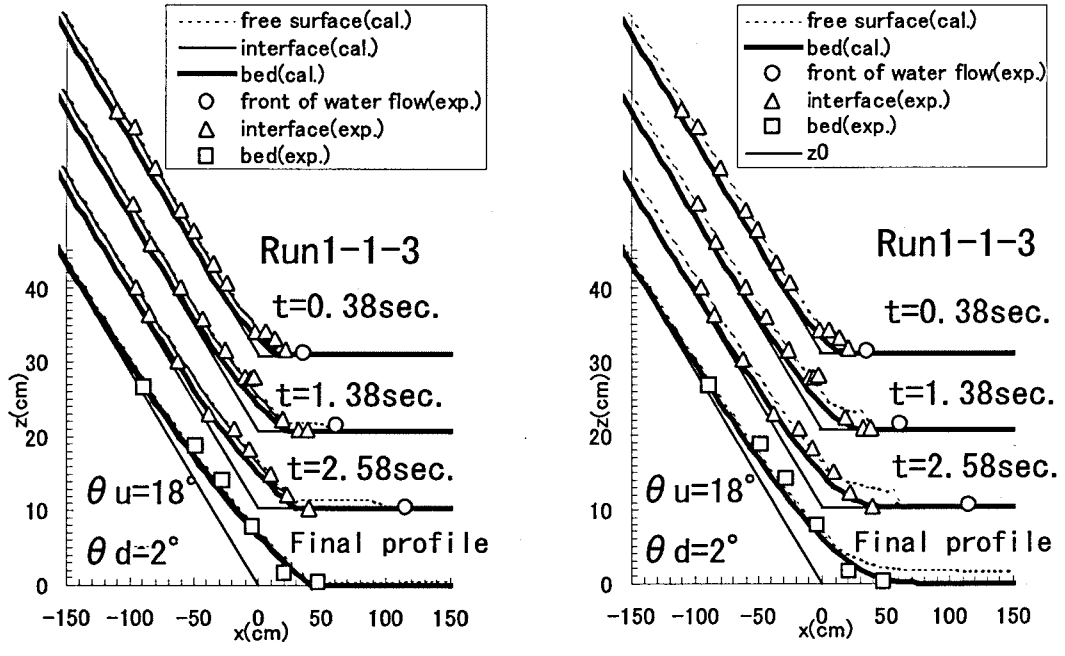

a)Two layer model (b)One layer model

Fig.8 Comparison between the deposition process obtained by flume experiment, Run1-1-3, and calculated results.

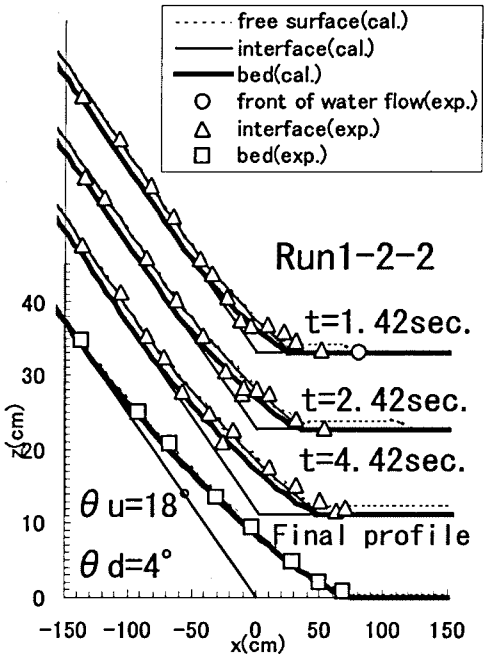

Fig.9 Comparison between the deposition process obtained by flume experiment, Run1-2-2, and calculated results.

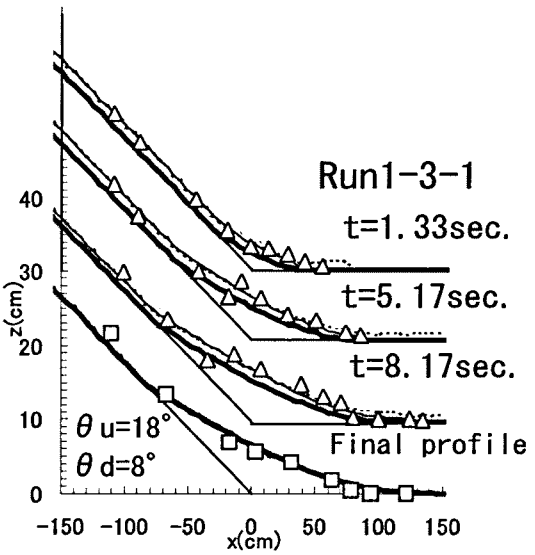

Fig.10 Comparison between the deposition process obtained by flume experiment, Run1-3-1, and calculated results.

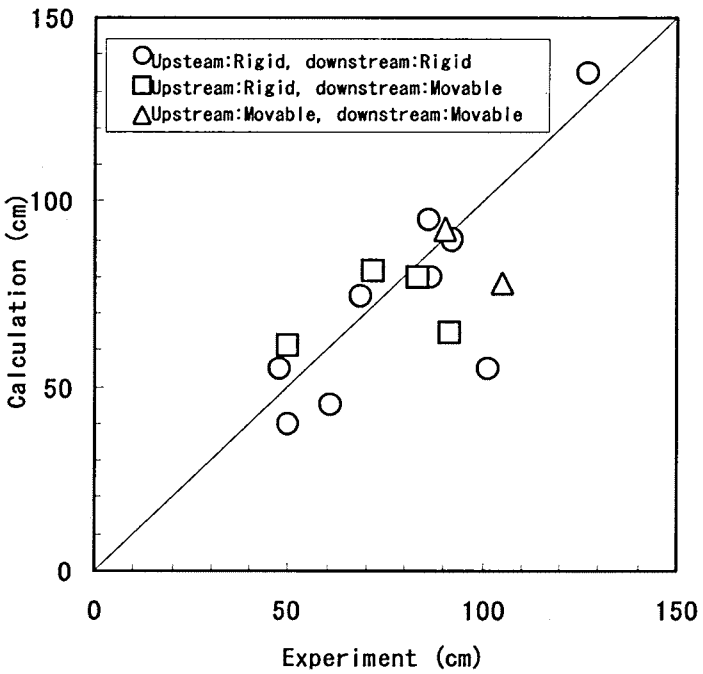

Fig.11 Comparison between the calculated and experimental values of traveling distance of sediment runoff by debris flows.

Fig.9 and Fig.10 show comparisons between the calculated results and experimental results under the condition for deceasing supply concentration at the inlet of the upper reach and increasing bed slope of downstream section in correspondence to the condition of Run1-1-3 respectively. The calculation results of the two layer model agree well with experimental results for the changes in bed slope and in supply concentrations. At the initial stage of deposition process observed in the experiment, there was a up-facing surface of sediment moving layer which forms step-like profile in a region of around a point of abrupt slope reducing. This profile dulled the its sharp shape, while it goes up, and it finally lapsed. This up-facing profile shape was remarkably observed in the experiment under the condition for making the upstream section to be a rigid bed. In the calculation results, the shape of the interface and the bed profiles were almost always straight or slightly curved linear. However, these discrepancy between experiments and calculations are appeared only in the initial stage and there are good agreement between calculated value and experimental value in the downstream from this step-like shape. And the effect of these discrepancy seems to be insignificant for the issues in the practical use such as the prediction of total amount and

traveling distance of sediment runoff in the field in which analyses by one-dimensional simulations are appropriate. Thus, usefulness of this model is clear from a comparison between experimental values and its values calculated of traveling distance of sediment runoff by debris flows as shown in Fig.11.

Experiment and analysis of erosion process of the debris flow

Experimental result and calculated are on the erosion process of debris flow are compared in Fig.12 for Run1-1-4. Fig.12 (a) shows only the calculated value of the flow in the upstream reach. In this experiment, after water-sediment mixture was supplied for 7.1 seconds, supply of sediment was stopped and only the water supply was continued for 14.4 seconds. At 2.7 second after the debris flow reaches the point of abrupt slope reducing, the front of a two-layer flow in the upstream reach migrated into the downstream reach. In the calculation results, the rate of re-erosion is slower than that observed in the experiment. The sediment moving layer in the calculation is propagated further upstream than that in the experimental result. Though there is such difference in the process for re-erosion, there are good agreement between the calculated value and experimental value of the final bed profile.

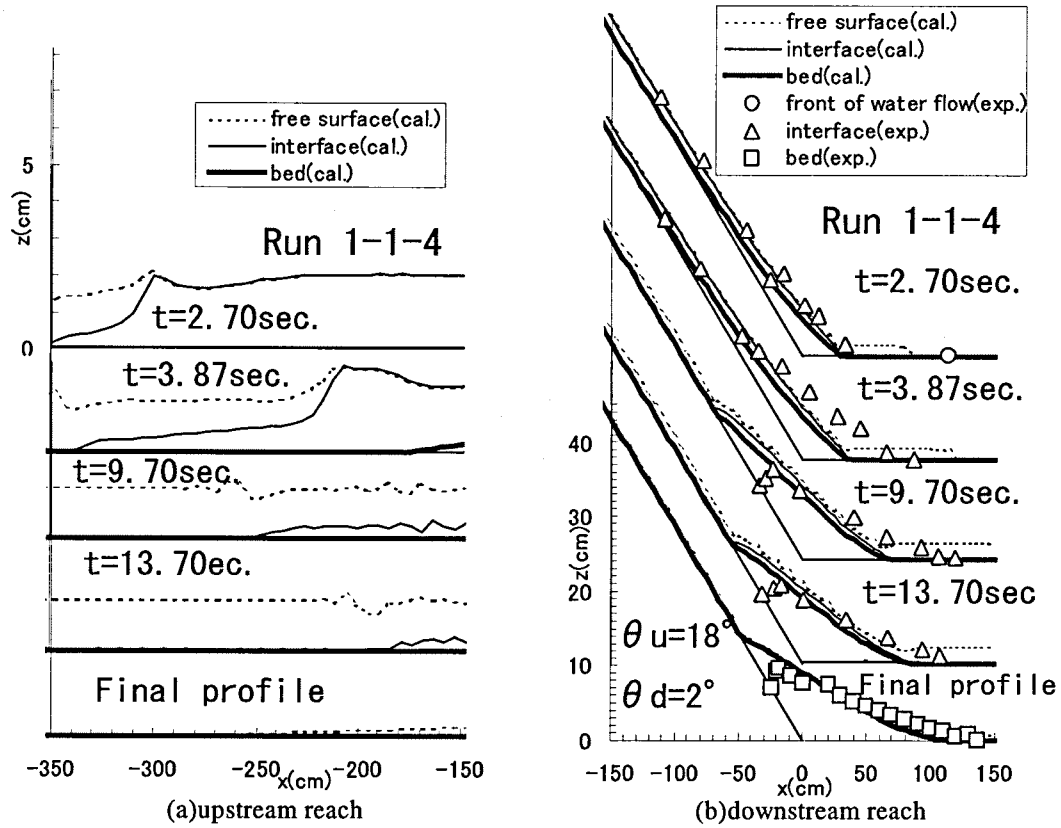

Fig.12 Comparison between the re-erosion process obtained by flume experiment, Run1-1-4, and its calculated results.

CONCLUSIONS

In this study, a new one-dimensional simulation model, a two-layer simulation model, was applied to deposition and erosion processes of debris flow in the channel with abrupt slope reducing, and the applicability was verified in comparison of results of simulation with the experimental ones. According to this model, it is possible to express the process for separation of the water flow layer with the deposition process and downward flow of debris flow.

Re-erosion process caused by the water flow after sedimentation by ceasing the debris flow often observed in the field can be reproduced by the experiment, and this process also was compared with calculation results by the two layer flow model. The two layer flow model proved to be possible to simulate smoothly and continuously the unsteady flow field including sediment moving layer and water flow layer without dividing the flowing sediment states such as fully dispersed debris flow, sediment sheet flow and bed-load.

REFERENCE

Ashida, K., Egashira, S., et al. (1984) The motion of a soil block released by slope failures, *Annual of Disaster Prevention Research Institute of Kyoto Univ.*, No. **28** B-2, 331-340(in Japanese).

Egashira, S., Ashida, K., et al. (1988) Mechanism of debris flow in open channel, *Annual Journal of Hydraulic Engineering*, JSCE, Vol.**32**, 485-490(in Japanese).

Egashira, S., Miyamoto, K., et al. (1997) Bed-load rate in view of two phase flow dynamics, *Annual Journal of Hydraulic Engineering, JSCE*, Vol.**41**, 789-794(in Japanese).

Hirano, M., Hashimoto, H., et al. (1997) Drag forces Solid-Liquid mixture flows on multiple rows of cylinders, *Annual Journal of Hydraulic Engineering, JSCE*, Vol.**41**, 699-704(in Japanese).

Itoh, T. and Egashira, S. (2001) Numerical simulation of debris flow at the San-Julian in 1999 sediment hazards, VENEZUELA, *PROCEEDINGS OF THE 56TH ANUUAL CONFERENCE OF THE JAPAN SOCIETY OF CIVIL ENGINEERS, 2*, p.128-129(in Japanese).

Takahama, J. and Miyamoto, K. (1995) Resistance principles and sediment discharge of high-density flow in steep channels, *Proceedings of the international Sabo symposium, Tokyo, Japan,* p.159-166.

Takahama, J., Fujita, Y., et al. (2000) Analysis method of transitional flow from debris flow to sediment sheet flow, *Annual Journal of Hydraulic Engineering, JSCE*, Vol.**44**, 683-686(in Japanese).

Takahama, J., Fujita, Y., et al. (2002) Two layer model for analysis of deposition and erosion processes of debris flow, *Annual Journal of Hydraulic Engineering, JSCE*, Vol.**46,** 677-682(in Japanese).

Takahashi, T. (1982): Study on the deposition of debris flows (3), *Annual of Disaster Prevention Research Institute of Kyoto Univ.*, No. **25** B-2, 327-348 (in Japanese).

Takahashi, T., Inoue, M., et al. (2000) Prediction of sediment runoff from a mountain water shed, *Annual Journal of Hydraulic Engineering, JSCE*, Vol.**44,** 717-722(in Japanese).